Commun. Comput. Phys.
doi: 10.4208/cicp.2019.js60.11

Vol. **26**, No. 5, pp. 1249-1273
November 2019

An Efficient Spectral Petrov-Galerkin Method for Nonlinear Hamiltonian Systems

Jing An[1], Waixiang Cao[2,*] and Zhimin Zhang[3,4]

[1] *School of Mathematical Sciences, Guizhou Normal University, Guiyang 550025, China.*
[2] *School of Mathematical Sciences, Beijing Normal University, Beijing 100875, China.*
[3] *Beijing Computational Science Research Center, Beijing 100193, China.*
[4] *Department of Mathematics, Wayne State University, Detroit, MI 48202, USA.*

Received 5 March 2019; Accepted (in revised version) 1 May 2019

Abstract. In this paper, an efficient spectral Petrov-Galerkin time-stepping method for solving nonlinear Hamiltonian systems is presented and studied. Conservation properties of the proposed method (including symplectic structure preserving and energy conservation) are discussed. Iterative algorithm on how to discretize the nonlinear term is introduced and the uniqueness, stability and convergence properties of the iterative algorithm are also established. Finally, numerical experiments are presented to verify the efficiency of our algorithm.

AMS subject classifications: 65M15, 65M70, 65N30

Key words: Nonlinear Hamiltonian system, spectral Petrov-Galerkin method, iterative algorithm, energy conservation, symplectic structure.

1 Introduction

Hamiltonian dynamical system was first introduced by Hamilton in 1824 as a general mathematical scheme for problems of geometrical optics. Since then, there is a growing interest of research and realization of the importance of Hamiltonian systems in many different areas such as classical mechanics, molecular dynamics, hydrodynamics, electrodynamics, plasma physics, relativity, astronomy, and so on [24, 25]. The numerical method or computational experiment is now considered as a very powerful technology and methodology for investigation and solving of the nonlinear Hamiltonian system since it is impossible to find exact solutions for most nonlinear Hamiltonian systems. A

*Corresponding author. *Email addresses:* aj154@163.com (J. An), caowx@bnu.edu.cn (W. Cao), zmzhang@csrc.ac.cn, zzhang@math.wayne.edu (Z. Zhang)

basic idea behind the design of numerical schemes is that they incorporate as many as possible properties of the original Hamiltonian dynamical system such as preservation of energy, preservation of momentum, symplecticity, reversibility in time, see, e.g. [2,22].

During the last decades, much work has been done in the field of designing momentum-conserving algorithms for Hamiltonian dynamical system, most important among which are symplectic algorithms and energy-momentum algorithms. Pioneering work on the symplectic geometry algorithm (that preserve the symplectic structure for Hamiltonian systems) can be found on Feng [10] and Ruth [28] and Channell [6]. Later, many different symplectic algorithms have been systematically developed and discussed, and many of them are Runge-Kutta methods. We refer to [5, 11–13, 21, 26, 29, 30] for an incomplete list of references in this field. Meanwhile, a number of algorithms have also been developed specifically for Hamiltonian systems to conserve the energy (see, e.g., [17, 18, 20, 34, 35]). For some highly oscillatory problems, energy preserving methods such as Störmer-Verlet-leapfrog methods, modulated Fourier expansion methods, have been developed to obtain long-time near-conservation of the total and oscillatory energies, see, e.g., [7, 8, 17, 18]. Given the importance of the Hamiltonian structure and energy-preserving properties of Hamiltonian systems, one might hope to find an algorithm which combines both of the desirable properties of the symplectic and energy-conservative algorithms. However, as is proved in [9, 38], there exists no energy preserving symplectic algorithm for general nonlinear Hamiltonian systems, and an energy-conservative algorithm would be at the expense of not being symplectic. Then we face a dilemma and have to choose between preserving energy and preserving symplectic structure. So far, it is not clear which algorithms should be preferred for a given application.

Due to the high order (spectral) accuracy, the spectral method has been widely used for numerical solutions of various differential equations, see, e.g., [3, 4, 14, 15, 31–33]. The spectral accuracy of the spectral method may provide us a new way to incorporate both properties of symplectic and energy-conservative algorithms for solving Hamiltonian systems in practice applications, with a negligible numerical error. Only recently, we present and study three kinds of efficient spectral methods (i.e., spectral Galerkin, Petrov-Galerkin, and collocation methods) for nonlinear Hamiltonian systems in [1]. We prove that the spectral Petrov-Galerkin method preserves the energy while both the spectral Gauss collocation and spectral Galerkin methods are energy conserving up to a spectral accuracy; and Petrov-Galerkin method preserves the symplectic structure up to a Gauss numerical quadrature error and the spectral Galerkin method preserves the symplectic structure up to a spectral accuracy error. In other words, in practice, all the three spectral methods are energy-preserving and symplectic structure up to a machine precision with a reasonable polynomial degree N.

The current work is the second in a series of study efficient algorithms for nonlinear Hamiltonian systems where the stability of the iterative algorithm and the application of the algorithm to various nonlinear Hamiltonian systems are under concern. Since the Gauss collocation method can be regarded as a special Runge-Kutta method, and

the spectral Galerkin method has been analyzed for some ordinary differential equations (see, e.g., [16]), we only focus our attention on the spectral Petrov-Galerkin method in this paper, which is a new method for solving Hamiltonian dynamical systems. We present two iterative algorithms to discretization the nonlinear term, and separately study the uniqueness, stability and convergence properties of the two iterative algorithms. The established stability results help us to understand and design iterative algorithms for different Hamiltonian functions better, and thus makes it more efficient for simulation. Furthermore, we applied our algorithms to various nonlinear Hamiltonian systems (including N-body problems) and compare the Petrov-Galerkin method with other classic symplectic methods. Numerical evidences show that the proposed Petrov-Galerkin method is more efficient than the symplectic methods (see Section 5).

The rest of this paper is organized as follows. In the next section, we present the spectral Petrov-Galerkin time-stepping method for nonlinear Hamiltonian systems. In Section 3, we analyze the conservation properties (including energy preserving and symplectic structure) of our algorithm. In Section 4, we propose two iterative algorithms to discretize the nonlinear Hamiltonian function and study the stability and convergence properties of the two iterative algorithms. Several numerical experiments are presented in Section 5 to demonstrate the accuracy and efficiency of our methods. Finally, in Section 6 we give some concluding remarks.

2 The Petrov-Galerkin method for Hamiltonian systems

In this paper, we present and study the spectral Petrov-Galerkin time-stepping method for the following canonical Hamiltonian systems

$$\frac{dp_i}{dt}=-\frac{\partial H}{\partial q_i},\quad \frac{dq_i}{dt}=\frac{\partial H}{\partial p_i},\qquad i=1,2,\cdots,n, \tag{2.1}$$

$$p_i(0)=p_{i0},\qquad q_i(0)=q_{i0},\qquad i=1,2,\cdots,n, \tag{2.2}$$

where $H=H(\mathbf{z})$ is a Hamiltonian function with

$$\mathbf{z}=(\mathbf{p},\mathbf{q}),\quad \mathbf{p}=(p_1,p_2,\cdots,p_n),\quad \mathbf{q}=(q_1,q_2,\cdots,q_n).$$

The spectral Petrov-Galerkin time-stepping method can be described as follows:

1. Choose a positive constant r, and use the Petrov-Galerkin method to solve the Hamiltonian system (2.1)-(2.2) and get a solution $(\mathbf{p},\mathbf{q})$ on $(0,r]$;
2. Solve the system (2.1)-(2.2) on $(r,2r]$ by the Petrov-Galerkin method with the initial condition taken as $(\mathbf{p}(r),\mathbf{q}(r))$ from the previous interval;
3. Repeat the process on the interval $[(m-1)r,mr],m>2$ and so on;
4. Obtain a global solution $(\mathbf{p},\mathbf{q})$ on the whole time domain $(0,T]$, $0<T\leq\infty$.

To demonstrate our algorithm clearly, we rewrite (2.1)-(2.2) into the following systems:

$$\frac{dp_i}{dt}=-\frac{\partial H}{\partial q_i},\quad \frac{dq_i}{dt}=\frac{\partial H}{\partial p_i},\quad t\in(mr,(m+1)r], \tag{2.3}$$

$$p_i(mr)=\tilde{p}_{i0},\quad q_i(mr)=\tilde{q}_{i0},\quad i=1,2,\cdots,n. \tag{2.4}$$

Here $\tilde{p}_{i0}$, $\tilde{q}_{i0}$ are the initial values obtained from the interval $[(m-1)r,mr]$ for all $m\geq 1$. Noticing that when $m=0$, we have $\tilde{p}_{i0}=p_{i0}$, $\tilde{q}_{i0}=q_{i0}$.

We denote by $\mathbb{P}_{N,m}$ the space of polynomial functions with a degree not more than N on $\tau_m=(mr,(m+1)r)$. Then the spectral Petrov-Galerkin method for (2.3)-(2.4) is to find $p_{iN},q_{iN}\in\mathbb{P}_{N,m}$ such that for all $v_{iN},w_{iN}\in\mathbb{P}_{N-1,m}$, $i\leq n$,

$$\left(\partial_t p_{iN},v_{iN}\right)_{\tau_m}=-\left(\frac{\partial H(p_{1N},\cdots,p_{nN};q_{1N},\cdots,q_{nN})}{\partial q_{iN}},v_{iN}\right)_{\tau_m},\quad p_{iN}(mr)=\tilde{p}_{i0}, \tag{2.5}$$

$$\left(\partial_t q_{iN},w_{iN}\right)_{\tau_m}=\left(\frac{\partial H(p_{1N},\cdots,p_{nN};q_{1N},\cdots,q_{nN})}{\partial p_{iN}},w_{iN}\right)_{\tau_m},\quad q_{iN}(mr)=\tilde{q}_{i0}, \tag{2.6}$$

where $(u,v)_{\tau_m}=\int_{mr}^{(m+1)r}(uv)(t)dt$.

Note that the time step size r is fixed in our numerical scheme. If the convergence of our algorithm is achieved by decreasing r and increasing N, then the numerical scheme (2.5)-(2.6) is the same as the hp-version of the continuous Galerkin time-stepping method proposed in [37]. To ensure the wellposedness of (2.5)-(2.6), r should satisfy some stable condition. Here we omit the discussion of the existence and uniqueness of numerical solution and refer to [37] for more detailed information.

3 Conservation properties

One of the important properties of Hamiltonian systems is that the Hamiltonian is conserved along trajectories. That is,

$$H(\mathbf{z}(t_M))=H(\mathbf{z}(t_0)).$$

Another important feature or property of the Hamiltonian system is the symplectic structure. That is, the Jacobi matrix of the transformation $(\frac{\partial \mathbf{z}}{\partial \mathbf{z}_0})$ satisfies

$$\left(\frac{\partial \mathbf{z}}{\partial \mathbf{z}_0}\right)^T J\left(\frac{\partial \mathbf{z}}{\partial \mathbf{z}_0}\right)=J,\quad J=\begin{pmatrix}\mathbf{0} & -I_n\\ I_n & \mathbf{0}\end{pmatrix}. \tag{3.1}$$

Here I_n denotes the $n\times n$ identity matrix, and $\mathbf{z}_0=(p_{10},\cdots,p_{n0};\,q_{10},\cdots,q_{n0})$.

The conservation properties (symplectic structure and energy preserving) of the spectral Petrov-Galerkin method has been studied and discussed in [1]. For the sake of completeness, we describe the conservation properties of the spectral Petrov-Galerkin method as follows.

Theorem 3.1. *Let*

$$\mathbf{z}_N=(\mathbf{p}_N,\mathbf{q}_N),\quad \mathbf{p}_N=(p_{1N},\cdots,p_{nN}),\quad \mathbf{q}_N=(q_{1N},\cdots,q_{nN}). \tag{3.2}$$

The Petrov-Galerkin method preserves the energy exactly, i.e.,

$$H(\mathbf{z}_N(t_M))=H(\mathbf{z}_N(t_0)). \tag{3.3}$$

Furthermore, if $\nabla H\in C^s(0,T)$, *then*

$$\left(\frac{\partial \mathbf{z}_N}{\partial \mathbf{z}_0}\right)^T J\left(\frac{\partial \mathbf{z}_N}{\partial \mathbf{z}_0}\right)=J+\mathcal{O}(N^{-s}). \tag{3.4}$$

Proof. First, (3.3) follows by adding the two equations (2.5)-(2.6) together and taking $(v_{iN},w_{iN})=(-\partial_t q_{iN},\partial_t p_{iN})$, and then summing up all i from 1 to n.

To show (3.4), we relate the spectral Petrov-Galerkin method with the Gauss collocation method which is a well-known symplectic scheme, and then use the relationship between the two numerical methods to study the symplectic structure conservation property of the spectral Petrov-Galerkin method.

In each element τ_m, we denote by $s_{m,j}$, $\omega_{m,j}$, $j\le N$ the N Gauss points and Gauss weights, and $\psi_j\in\mathbb{P}_{N-1,m}$ the corresponding Lagrange basis function associated with the Gauss points $s_{m,j}$, $j\le N$. By taking $v_{iN}=\psi_j$, $w_{iN}=\psi_j$ in (2.5)-(2.6) and using the fact that the Gauss quadrature is exact for all polynomials of degree not more than $2N-1$, we obtain

$$\partial_t p_{iN}(s_{m,j})=-\frac{\partial H(z_N(s_{m,j}))}{\partial q_{iN}}-\frac{1}{\omega_{m,j}}\bar{E}_{ij},\quad \partial_t q_{iN}(s_{m,j})=\frac{\partial H(z_N(s_{m,j}))}{\partial p_{iN}}+\frac{1}{\omega_{m,j}}\tilde{E}_{ij}. \tag{3.5}$$

where both $\bar{E}_{ij}$ and $\tilde{E}_{ij}$ are Gauss numerical quadrature errors. To be more precise,

$$\bar{E}_{ij}=\Big(\frac{\partial H(z_N)}{\partial q_{iN}},\psi_j\Big)-\frac{\partial H(z_N(s_{m,j}))}{\partial q_{iN}}\omega_{m,j},\quad \tilde{E}_{ij}=\Big(\frac{\partial H(z_N)}{\partial p_{iN}},\psi_j\Big)-\frac{\partial H(z_N(s_{m,j}))}{\partial p_{iN}}\omega_{m,j}.$$

Eq. (3.5) indicates that the spectral Petrov-Galerkin method is almost equivalent to the Gauss collocation method up to a Gauss numerical quadrature error. Moreover, if $\nabla H\in C^s(0,T)$, then there exists a constant c independent of N such that

$$|\bar{E}_{ij}|+|\tilde{E}_{ij}|\le cN^{-s},\quad \forall 1\le i\le n.$$

Let

$$y=\frac{\partial z_N}{\partial z_0},\quad y_1=\frac{\partial z_N(t_{m+1})}{\partial z_0},\quad y_0=\frac{\partial z_N(t_m)}{\partial z_0},\quad t_m=mr.$$

Following the same argument as that for the Gauss collocation method in [19], we get

$$\begin{aligned} y_1^T J y_1 - y_0^T J y_0 &= \int_{t_m}^{t_{m+1}} \frac{d}{dx}(y^T J y)dx = \sum_{j=1}^{N} \left((\frac{dy}{dx})^T J y + y^T J \frac{dy}{dx} \right)(s_j)\omega_j \\ &= \sum_{j=1}^{N} \Big(\big(y^T (\nabla^2 H)^T J^{-T} \omega_j + E_j^T \big) J y + y^T J \big(E_j + J^{-1} \nabla^2 H y \omega_j \big) \Big)(s_j) \\ &= \sum_{j=1}^{N} \Big(E_j^T J y + y^T J E_j \Big)(s_j) = \mathcal{O}(N^{-s}). \end{aligned}$$

Here $E_j = \frac{\partial}{\partial z_0}(-\bar{E}_{1j}, \cdots, -\bar{E}_{nj}; \tilde{E}_{1j}, \cdots, \tilde{E}_{nj})^T$, $\nabla^2 H = \nabla^2 H(z_N)$ denotes the Hessian matrix of $H(z_N)$, and in the second step, we have used (3.5) and the fact that $J^{-T} J = -JJ^{-1} = -I_{2n}$. Consequently, for all $t \in (0, T]$,

$$\left(\frac{\partial z_N}{\partial z_0} \right)^T J \left(\frac{\partial z_N}{\partial z_0} \right)(t) = \left(\frac{\partial z_N}{\partial z_0} \right)^T J \left(\frac{\partial z_N}{\partial z_0} \right)(0) + \mathcal{O}(tN^{-s}) = J + \mathcal{O}(N^{-s}).$$

Then (3.4) follows. The proof is complete. □

As we may observe, the error bounds N^{-s} in (3.4) is considered as spectral accuracy. In other words, we are able to control the error to the machine epsilon, i.e., 10^{-15} with a reasonable N, which indicates that our algorithm is in practice symplectic structure preserving once the error reaches the machine precision. In this sense (up to a spectral accuracy or a machine precision), our algorithm preserves the symplectic structure and energy simultaneously in practical applications.

4 Stability analysis

4.1 Iterative algorithms

This section is dedicated to studying the iterative algorithm for (2.5)-(2.6). To discretize the nonlinear terms $\frac{\partial H}{\partial q_{iN}}$ and $\frac{\partial H}{\partial p_{iN}}$, we present two different methods. The first one is to linearize $\frac{\partial H}{\partial q_{iN}}$ and $\frac{\partial H}{\partial p_{iN}}$ directly, i.e.,

$$\begin{aligned} \big(\partial_t p_{iN}^{k+1}, v_{iN} \big)_{\tau_m} &= -\left(\frac{\partial H(p_{1N}^k, \cdots, p_{nN}^k; q_{1N}^k, \cdots, q_{nN}^k)}{\partial q_{iN}}, v_{iN} \right)_{\tau_m}, \\ \big(\partial_t q_{iN}^{k+1}, w_{iN} \big)_{\tau_m} &= \left(\frac{\partial H(p_{1N}^k, \cdots, p_{nN}^k; q_{1N}^k, \cdots, q_{nN}^k)}{\partial p_{iN}}, w_{iN} \right)_{\tau_m}. \end{aligned} \tag{4.1}$$

The other one is to divide $\frac{\partial H}{\partial q_{iN}}$ and $\frac{\partial H}{\partial p_{iN}}$ into linear and nonlinear parts $\frac{\partial H}{\partial p_{iN}}=\mathcal{L}_{p_{iN}}+\mathcal{N}_{p_{iN}}$, $\frac{\partial H}{\partial q_{iN}}=\mathcal{L}_{q_{iN}}+\mathcal{N}_{q_{iN}}$, and then perform the following iterative scheme:

$$\begin{aligned}&\left(\partial_t p_{iN}^{k+1},v_{iN}\right)_{\tau_m}=-(\mathcal{L}_{q_{iN}}^{k+1},v_{iN})_m-(\mathcal{N}_{q_{iN}}^{k},v_{iN})_{\tau_m},\\&\left(\partial_t q_{iN}^{k+1},w_{iN}\right)_{\tau_m}=(\mathcal{L}_{p_{iN}}^{k+1},w_{iN})_m+(\mathcal{N}_{p_{iN}}^{k},w_{iN})_{\tau_m},\quad i=1,2,\cdots,n,\end{aligned}\tag{4.2}$$

where

$$\begin{aligned}&\mathcal{L}_{q_{iN}}^{k+1}=\mathcal{L}_{q_{iN}}(p_{1N}^{k+1},\cdots,p_{nN}^{k+1};q_{1N}^{k+1},\cdots,q_{nN}^{k+1}),\\&\mathcal{N}_{q_{iN}}^{k}=\mathcal{N}_{q_{iN}}(p_{1N}^{k},\cdots,p_{nN}^{k};q_{1N}^{k},\cdots,q_{nN}^{k}).\end{aligned}$$

To compute the nonlinear integration terms appeared in (4.1) or (4.2), we use the $2N$-point Gauss numerical quadrature formulae in our numerical experiments, which indicates that in the numerical sense, the spectral Galerkin method is equivalent to the $2N$ Gauss collocation method proposed in [16]. Furthermore, efficient numerical experiments for the second iterative scheme has been presented and studied in [1] while the uniqueness of the solution and convergence analysis of the iterative algorithm remain open. In the following, we shall study the uniqueness and convergence of the iterative algorithms (4.1) and (4.2).

4.2 Analysis for the iterative algorithm (4.1)

We begin with some preliminaries.

First, let ϕ_n and L_n be the standard Lobatto and Legendre polynomials on $[-1,1]$ respectively. To be more precise,

$$\phi_0(s)=\frac{1-s}{2},\quad \phi_1(s)=\frac{1+s}{2},\quad \phi_n(s)=\int_{-1}^{s}L_{n-1}(\tau)d\tau=\frac{1}{2n-1}(L_n-L_{n-2})(s),\quad n\geq 2.\tag{4.3}$$

Denote by $-1<s_1<s_2<\cdots<s_N<1$ the Gauss points of degree N, and $\{\omega_j\}_{j=1}^N$ the corresponding weights of Gauss numerical quadrature. By a scaling from $[-1,1]$ to $[mr,(m+1)r]$, we get the shift Gauss points and weights on $[mr,(m+1)r]$, which are denoted by $s_{m,j},\omega_{m,j}$, $j\leq N$.

Second, for any function v, let $\pi_N v$ be the L^2 projection of v. That is.

$$(\pi_N v,w)_{\tau_m}=(v,w)_{\tau_m},\quad \forall w\in\mathbb{P}_{N,m}.$$

In each interval $[mr,(m+1)r]$, we denote by $\psi_j\in\mathbb{P}_{N-1,m}$ the Lagrange interpolation function associated with the N Gauss points $s_{m,j}$. Then we have from (4.1)

$$\begin{aligned}&(\partial_t p_{iN}^{k+1},\psi_j)_{\tau_m}=-(H_{q_{iN}}(\mathbf{p}_N^k,\mathbf{q}_N^k),\psi_j)_{\tau_m}=-(\pi_{N-1}H_{q_{iN}}(\mathbf{p}_N^k,\mathbf{q}_N^k),\psi_j)_{\tau_m},\\&(\partial_t q_{iN}^{k+1},\psi_j)_{\tau_m}=(H_{p_{iN}}(\mathbf{p}_N^k,\mathbf{q}_N^k),\psi_j)_{\tau_m}=(\pi_{N-1}H_{p_{iN}}(\mathbf{p}_N^k,\mathbf{q}_N^k),\psi_j)_{\tau_m}.\end{aligned}$$

Note that N points Gauss numerical quadrature is exact for all polynomial of degree not more than $2N-1$, we have

$$\partial_t p_{iN}^{k+1}(s_{m,j})\omega_{m,j}=\sum_{l=1}^{N}(\partial_t p_{iN}^{k+1}\psi_j)(s_{m,l})\omega_{m,l}=-(\pi_{N-1}H_{q_{iN}}(\mathbf{p}_N^k,\mathbf{q}_N^k))(s_{m,j})\omega_{m,j},\quad j\leq N.$$

For any function $v\in\mathbb{P}_{N,m}$, multiplying both sides of the above equation by $v(s_{m,j})\omega_{m,j}$ and then summing up all j yields

$$(\partial_t p_{iN}^{k+1},v)_{\tau_m}=-(\pi_{N-1}H_{q_{iN}}(\mathbf{p}_N^k,\mathbf{q}_N^k),v)_{\tau_m},\quad \forall v\in\mathbb{P}_{N,m}. \tag{4.4}$$

Similarly, we get

$$(\partial_t q_{iN}^{k+1},w)_{\tau_m}=(\pi_{N-1}H_{p_{iN}}(\mathbf{p}_N^k,\mathbf{q}_N^k),w)_{\tau_m},\quad \forall w\in\mathbb{P}_{N,m}. \tag{4.5}$$

For any functions $\mathbf{z}_1$ and $\mathbf{z}_2$, suppose that the Hamiltonian function H satisfies

$$|H_{p_i}(\mathbf{z}_1)-H_{p_i}(\mathbf{z}_2)|\leq\kappa|\mathbf{z}_1-\mathbf{z}_2|,\quad |H_{q_i}(\mathbf{z}_1)-H_{q_i}(\mathbf{z}_2)|\leq\kappa|\mathbf{z}_1-\mathbf{z}_2|,\quad \forall i\leq n \tag{4.6}$$

for some positive constant κ. Here for any vector $\mathbf{z}_1=(x_1,\cdots,x_n)^T$, $|\mathbf{z}_1|=\sum_{i=1}^n|x_i|$.

Theorem 4.1. *Assume that the Hamiltonian functions H_p,H_q are Lipschitz continuous. That is,* (4.6) *is satisfied for some $\kappa>0$. Then given a $\mathbf{z}_N^k=(\mathbf{p}_N^k,\mathbf{q}_N^k)$, the iterative algorithm* (4.1) *admits a unique solution $(\mathbf{p}_N^{k+1},\mathbf{q}_N^{k+1})$ provided that $8\kappa rn\leq\beta<1$ for some positive β. Moreover, suppose $\{\mathbf{z}_N^k\}_{k=1}^{\infty}$ is the sequence generated from the iterative algorithm* (4.1)*, then the sequence $\{\mathbf{z}_N^k\}$ is convergent to $\mathbf{z}_N$ with the following estimate:*

$$\|\mathbf{z}_N^k-\mathbf{z}_N\|_{[0,T]}\leq\left(\frac{\beta}{1-\beta}\right)^k\|\mathbf{z}_N^1-\mathbf{z}_N^0\|_{[0,T]}. \tag{4.7}$$

Proof. Let

$$e_{p_i}^k=p_{iN}^{k+1}-p_{iN}^k,\quad e_{q_i}^k=q_{iN}^{k+1}-q_{iN}^k,\quad i\leq n.$$

By (4.4)-(4.5), we have

$$(\partial_t e_{p_i}^k,v)_{\tau_m}=-(\pi_{N-1}H_{q_{iN}}(\mathbf{p}_N^k,\mathbf{q}_N^k)-\pi_{N-1}H_{q_{iN}}(\mathbf{p}_N^{k-1},\mathbf{q}_N^{k-1}),v)_{\tau_m},\quad \forall v\in\mathbb{P}_{N,m}. \tag{4.8}$$

Let $\|v\|_{\tau_m}:=\left(\int_{\tau_m}v^2dt\right)^{\frac{1}{2}}$. On the one hand, we choose $v=\partial_t e_{p_i}^k$ in (4.8) to obtain

$$\begin{aligned}\|\partial_t e_{p_i}^k\|_{\tau_m}^2&\leq\int_{t_m}^{t_{m+1}}\left|\partial_t e_{p_i}^k(H_{q_{iN}}(\mathbf{z}_N^k)-H_{q_{iN}}(\mathbf{z}_N^{k-1}))\right|dt\\&\leq\kappa\|\partial_t e_{p_i}^k\|_{\tau_m}\sum_{i=1}^{n}(\|e_{p_i}^{k-1}\|_{\tau_m}+\|e_{q_i}^{k-1}\|_{\tau_m}).\end{aligned} \tag{4.9}$$

On the other hand, by choosing $v_N = 2e^k_{p_i}$ in (4.8) and using the fact that $e^k_{p_i}(mr) = 0$, we have for any $t_{m+1} = (m+1)r$

$$\begin{aligned}|e^k_{p_i}(t_{m+1})|^2 &= 2(\pi_{N-1}H_{q_{iN}}(\mathbf{p}^{k-1}_N, \mathbf{q}^{k-1}_N) - \pi_{N-1}H_{q_{iN}}(\mathbf{p}^k_N, \mathbf{q}^k_N), e^k_{p_i})_{\tau_m} \\ &\le 2\|e^k_{p_i}\|_{\tau_m}\|H_{q_{iN}}(\mathbf{p}^{k-1}_N, \mathbf{q}^{k-1}_N) - H_{q_{iN}}(\mathbf{p}^k_N, \mathbf{q}^k_N)\|_{\tau_m}. \end{aligned} \tag{4.10}$$

Note that for any $t \in \tau_m$,

$$\begin{aligned}|e^k_{p_i}(t)|^2 &= |e^k_{p_i}(t_{m+1})|^2 - \int_t^{t_{m+1}} \frac{d}{ds}(e^k_{p_i}(s))^2 ds \\ &\le |e^k_{p_i}(t_{m+1})|^2 + 2\kappa\|e^k_{p_i}\|_{\tau_m}\sum_{i=1}^n (\|e^{k-1}_{p_i}\|_{\tau_m} + \|e^{k-1}_{q_i}\|_{\tau_m}). \end{aligned} \tag{4.11}$$

Here in the last step, we have used (4.9). Integrating the above inequality with respect to t on the interval τ_m yields that

$$\|e^k_{p_i}\|^2_{\tau_m} \le r|e^k_{p_i}(t_{m+1})|^2 + 2\kappa r\|e^k_{p_i}\|_{\tau_m}\sum_{i=1}^n (\|e^{k-1}_{p_i}\|_{\tau_m} + \|e^{k-1}_{q_i}\|_{\tau_m}),$$

and thus

$$|e^k_{p_i}(t_{m+1})|^2 \ge \frac{1}{r}\|e^k_{p_i}\|^2_{\tau_m} - 2\kappa\|e^k_{p_i}\|_{\tau_m}\sum_{i=1}^n (\|e^{k-1}_{p_i}\|_{\tau_m} + \|e^{k-1}_{q_i}\|_{\tau_m}). \tag{4.12}$$

Substituting the above inequality into (4.10) gives that

$$\|e^k_{p_i}\|^2_{\tau_m} \le 2\kappa r\|e^k_{p_i}\|_{\tau_m}\sum_{i=1}^n (\|e^{k-1}_{p_i}\|_{\tau_m} + \|e^{k-1}_{q_i}\|_{\tau_m}) + 2r\|e^k_{p_i}\|_{\tau_m}\|H_{q_{iN}}(\mathbf{z}^{k-1}_N) - H_{q_{iN}}(\mathbf{z}^k_N)\|_{\tau_m}.$$

Consequently,

$$\|e^k_{p_i}\|_{\tau_m} \le 2\kappa r\sum_{i=1}^n (\|e^{k-1}_{p_i}\|_{\tau_m} + \|e^{k-1}_{q_i}\|_{\tau_m}) + 2r\|H_{q_{iN}}(\mathbf{z}^{k-1}_N) - H_{q_{iN}}(\mathbf{z}^k_N)\|_{\tau_m}.$$

In light of (4.6), we have

$$\begin{aligned}\|H_{q_{iN}}(\mathbf{z}^{k-1}_N) - H_{q_{iN}}(\mathbf{z}^k_N)\|_{\tau_m} &\le \kappa\left(\int_{t_m}^{t_{m+1}} |\mathbf{z}^k_N - \mathbf{z}^{k-1}_N|^2 dt\right)^{\frac{1}{2}} \\ &= \kappa\left(\int_{t_m}^{t_{m+1}} \left(\sum_{i=1}^n |e^{k-1}_{p_i}| + |e^{k-1}_{q_i}|\right)^2 dt\right)^{\frac{1}{2}} \\ &\le \kappa\sum_{i=1}^n (\|e^{k-1}_{p_i}\|_{\tau_m} + \|e^{k-1}_{q_i}\|_{\tau_m}). \end{aligned} \tag{4.13}$$

Here in the last step, we have used the triangle inequality of the L^2 norm, i.e.,

$$\|v_1+v_2+\cdots+v_n\|_{\tau_m}=\|v_1\|_{\tau_m}+\|v_2\|_{\tau_m}+\cdots+\|v_n\|_{\tau_m}.$$

Consequently,

$$\|e^k_{p_i}\|_{\tau_m}\leq 4\kappa r\sum_{i=1}^{n}(\|e^{k-1}_{p_i}\|_{\tau_m}+\|e^{k-1}_{q_i}\|_{\tau_m}).$$

Following the same argument, we have

$$\|e^k_{q_i}\|_{\tau_m}\leq 4\kappa r\sum_{i=1}^{n}(\|e^{k-1}_{p_i}\|_{\tau_m}+\|e^{k-1}_{q_i}\|_{\tau_m}).$$

Summing up all i from 1 to n yields

$$\sum_{i=1}^{n}(\|e^k_{p_i}\|_{\tau_m}+\|e^k_{q_i}\|_{\tau_m})\leq 8\kappa rn\sum_{i=1}^{n}(\|e^{k-1}_{p_i}\|_{\tau_m}+\|e^{k-1}_{q_i}\|_{\tau_m}).$$

Therefore, if $8\kappa rn\leq\beta<1$ for some positive constant $\beta<1$, then

$$\|\mathbf{z}^{k+1}_N-\mathbf{z}^k_N\|_{\tau_m}:=\sum_{i=1}^{n}\left(\|e^k_{p_i}\|_{\tau_m}+\|e^k_{q_i}\|_{\tau_m}\right)\leq\beta\|\mathbf{z}^k_N-\mathbf{z}^{k-1}_N\|_{\tau_m}.$$

Summing up all m, we have

$$\|\mathbf{z}^{k+1}_N-\mathbf{z}^k_N\|_{[0,T]}\leq\beta\|\mathbf{z}^k_N-\mathbf{z}^{k-1}_N\|_{[0,T]},$$

and thus

$$\|\mathbf{z}^{k+1}_N-\mathbf{z}^k_N\|_{[0,T]}\to 0,\quad \text{as } k\to\infty,$$

which indicates the existence and uniqueness of the global solution of (4.1). Then the sequence $\{\mathbf{z}^k_N\}$ is convergent to its limits $\mathbf{z}_N$. Furthermore, following the same argument, we obtain

$$\begin{aligned}\|\mathbf{z}^{k+1}_N-\mathbf{z}_N\|_{[0,T]}&\leq\beta\|\mathbf{z}^k_N-\mathbf{z}_N\|_{[0,T]}\leq\frac{\beta}{1-\beta}\|\mathbf{z}^k_N-\mathbf{z}^{k+1}_N\|_{[0,T]}\\&\leq\left(\frac{\beta}{1-\beta}\right)^{k+1}\|\mathbf{z}^1_N-\mathbf{z}^0_N\|_{[0,T]}.\end{aligned}$$

This finishes our proof. □

4.3 Analysis for the iterative algorithm (4.2)

Theorem 4.2. *Assume that the nonlinear part of the Hamiltonian function satisfies* (4.6) *for some* $\kappa>0$, *and the linear parts in* (4.2) *has the following expression*

$$(\mathcal{L}^{k+1}_{q_{iN}},v_{iN})_{\tau_m}=\sum_{j=1}^{n}a_{ij}(p^{k+1}_{jN},v_{iN})_m+b_{ij}(q^{k+1}_{jN},v_{iN})_{\tau_m},$$
$$(\mathcal{L}^{k+1}_{p_{iN}},v_{iN})_{\tau_m}=\sum_{j=1}^{n}c_{ij}(p^{k+1}_{jN},v_{iN})_m+d_{ij}(q^{k+1}_{jN},v_{iN})_{\tau_m}.$$

Let $c_0=\max(|a_{i,j}|,|b_{i,j}|)$ *and* $c_1=\max(|c_{i,j}|,|d_{i,j}|)$. *Then given a* $\mathbf{z}^k_N=(\mathbf{p}^k_N,\mathbf{q}^k_N)$, *the iterative algorithm* (4.2) *admits a unique solution* $(\mathbf{p}^{k+1}_N,\mathbf{q}^{k+1}_N)$ *provided that* $4rn(2\kappa+c_0+c_1)\le\beta<1$ *for some constant* β. *Moreover, suppose* $\{\mathbf{z}^k_N\}_{k=1}^{\infty}$ *is the sequence generated from the iterative algorithm* (4.2), *then the sequence* $\{\mathbf{z}^k_N\}$ *is convergent to* $\mathbf{z}_N$ *with*

$$\|\mathbf{z}^k_N-\mathbf{z}_N\|_{[0,T]}\le\left(\frac{\beta}{1-\beta}\right)^k\|\mathbf{z}^1_N-\mathbf{z}^0_N\|_{[0,T]}.$$

Proof. Following the same argument as what we did in (4.8), there holds for all $v\in\mathbb{P}_{N,m}$ that

$$(\partial_t e^k_{p_i},v)_{\tau_m}=-\sum_{j=1}^{n}(a_{ij}e^k_{p_i}+b_{ij}e^k_{q_i},v)_{\tau_m}+(\pi_{N-1}\mathcal{N}_{q_{iN}}(\mathbf{p}^{k-1}_N,\mathbf{q}^{k-1}_N)-\pi_{N-1}\mathcal{N}_{q_{iN}}(\mathbf{p}^k_N,\mathbf{q}^k_N),v)_{\tau_m}. \tag{4.14}$$

Choosing $v_N=2e^k_{p_i}$ and using the equation $e^k_{p_i}(t_m)=0$ and (4.13) yields

$$|e^k_{p_i}(t_{m+1})|^2\le 2(c_0+\kappa)\|e^k_{p_i}\|_{\tau_m}\sum_{i=1}^{n}(\|e^{k-1}_{p_i}\|_{\tau_m}+\|e^{k-1}_{q_i}\|_{\tau_m}). \tag{4.15}$$

Similarly, we choose $v=\partial_t e^k_{p_i}$ in (4.14) to obtain

$$\|\partial_t e^k_{p_i}\|^2_{\tau_m}\le(c_0+\kappa)\|\partial_t e^k_{p_i}\|_{\tau_m}\sum_{i=1}^{n}(\|e^{k-1}_{p_i}\|_{\tau_m}+\|e^{k-1}_{q_i}\|_{\tau_m}),$$

which yields, together with the first inequality of (4.11),

$$|e^k_{p_i}(t)|^2\le|e^k_{p_i}(t_{m+1})|^2+2\|e^k_{p_i}\|_{\tau_m}\|\partial_t e^k_{p_i}\|_{\tau_m}\le 4(c_0+\kappa)\|e^k_{p_i}\|_{\tau_m}\sum_{i=1}^{n}(\|e^{k-1}_{p_i}\|_{\tau_m}+\|e^{k-1}_{q_i}\|_{\tau_m}).$$

Integrating the above inequality with respect to t on the interval τ_m, we have

$$\|e^k_{p_i}\|^2_{\tau_m}\le 4r(c_0+\kappa)\|e^k_{p_i}\|_{\tau_m}\sum_{i=1}^{n}(\|e^{k-1}_{p_i}\|_{\tau_m}+\|e^{k-1}_{q_i}\|_{\tau_m}),$$

and thus

$$\|e_{p_i}^k\|_{\tau_m} \leq 4r(c_0+\kappa)\sum_{i=1}^{n}(\|e_{p_i}^{k-1}\|_{\tau_m}+\|e_{q_i}^{k-1}\|_{\tau_m}).$$

Similarly, we derive

$$\|e_{q_i}^k\|_{\tau_m} \leq 4r(c_1+\kappa)\sum_{i=1}^{n}(\|e_{p_i}^{k-1}\|_{\tau_m}+\|e_{q_i}^{k-1}\|_{\tau_m}).$$

Summing up all i from 1 to n, we get

$$\sum_{i=1}^{n}(\|e_{p_i}^k\|_{\tau_m}+\|e_{q_i}^k\|_{\tau_m}) \leq 4rn(c_0+c_1+2\kappa)\sum_{i=1}^{n}(\|e_{p_i}^{k-1}\|_{\tau_m}+\|e_{q_i}^{k-1}\|_{\tau_m}).$$

Therefore, if $4rn(2\kappa+c_0+c_1) \leq \beta < 1$, we have

$$\sum_{i=1}^{n}(\|e_{p_i}^k\|_{\tau_m}+\|e_{q_i}^k\|_{\tau_m}) \leq \beta\sum_{i=1}^{n}(\|e_{p_i}^{k-1}\|_{\tau_m}+\|e_{q_i}^{k-1}\|_{\tau_m}).$$

Then the solution of the iterative algorithm (4.2) is unique and the sequence is convergent. The rest of the proof is similar to that of Theorem 4.1. This finishes our proof. □

In [1], we study the error estimate of the spectral Petrov-Galerkin method for the nonlinear Hamiltonian system (2.1)-(2.2) and prove that the numerical solution converges exponentially with respect to N. While for the iterative scheme (4.1)-(4.2), as we may observe from Theorems 4.1-4.2, the error estimate is dependent upon both the polynomial degree N and the number of the iterative k. In other words, the number of the iterative k has effect on the convergence speed.

5 Numerical experiments

In this section, we perform some numerical experiments to present the efficiency, the energy-preserving property of the algorithm proposed in Section 4. If not otherwise stated, the iterative scheme is chosen in the same way as in (4.2). We operate our programs in MATLAB 2016b.

Example 5.1. Threefold symmetry Hamiltonian system [12, 27]. Consider a $k-$fold rotational symmetry system in phase plane with Hamiltonian

$$H_k(p;q) = \sum_{j=1}^{k}\cos\left(p\cos\left(\frac{2\pi j}{k}\right)+q\sin\left(\frac{2\pi j}{k}\right)\right).$$

For comparing with the numerical results in [27], we also consider the system of nonlinear ordinary differential equations for the Hamiltonian $H_3(p,q)$, i.e.,

$$p'(t)=-\frac{\partial H}{\partial q}=\frac{\sqrt{3}}{2}\sin\Big(-\frac{1}{2}p+\frac{\sqrt{3}}{2}q\Big)+\frac{\sqrt{3}}{2}\sin\Big(\frac{1}{2}p+\frac{\sqrt{3}}{2}q\Big), \tag{5.1}$$

$$q'(t)=\frac{\partial H}{\partial p}=-\sin(p)+\frac{1}{2}\sin\Big(-\frac{1}{2}p+\frac{\sqrt{3}}{2}q\Big)-\frac{1}{2}\sin\Big(\frac{1}{2}p+\frac{\sqrt{3}}{2}q\Big), \tag{5.2}$$

with initial condition $p(0)=\pi$, $q(0)=0$. Note that $H(0)=-1$ and $(p,q)=(\pi,-\frac{\sqrt{3}}{3}\pi)$ is a exact steady-state solution. Since there is no linear term in the formula of the Hamiltonian function, then both the coefficients c_0 and c_1 in Theorem 4.2 equal to zero. Furthermore, the coefficient κ in (4.6) can be chosen as the maximal value of the second derivative of $H(p,q)$, i.e.,

$$\kappa=\max\Big(\frac{\partial^2 H}{\partial p^2},\frac{\partial^2 H}{\partial q^2},\frac{\partial^2 H}{\partial q\partial p}\Big).$$

In this case, a direct calculation yields $\kappa=\frac{3}{2}$. As indicated by Theorem 4.2, r should be chosen such that

$$r\leq\frac{1}{8n\kappa}=\frac{1}{12}.$$

In other words, when $0\leq r\leq\frac{1}{12}$, the iterative scheme (4.2) is stable.

In our numerical experiments, we choose $r=0.5$ and we plot in Fig. 1 the graphs of p_N,q_N with respect to different time t for $N=20$, 30. As we may observe, the numerical solution (p_N,q_N) is almost a constant as t increases, which indicates that our algorithm is stable. To show the convergence property of our algorithm, we plot in Fig. 2 the error curves between the numerical solution (p_N,q_N) and the exact solution $(\pi,-\frac{\sqrt{3}}{3}\pi)$ with respect to time t for $N=30$, from which we see that the approximation error can reach as high as the machine precision 10^{-15} even for large t, i.e., t=1000. Therefore, the numerical solution is indeed convergent to the exact solution $(\pi,-\frac{\sqrt{3}}{3}\pi)$, which indicates that our algorithm is convergent and preserves the energy.

In [27], the authors proposed a Lobatto spectral collocation method and a symplectic method specially designed for the threefold symmetry system. To show the efficiency of our algorithm, we compare in Table 1 the CPU time used for the spectral Petrov-Galerkin method with that for the Lobatto spectral collocation method and the symplectic method proposed in [27]. The numerical scheme of the symplectic method is as follows:

$$P_1=p^k+\frac{\sqrt{3}}{4}r\sin\Big(\frac{p^k}{2}+\frac{\sqrt{3}q^k}{2}\Big),\quad Q_1=q^k-\frac{1}{4}r\sin\Big(\frac{p^k}{2}+\frac{\sqrt{3}q^k}{2}\Big),$$

$$P_2=P_1-\frac{\sqrt{3}}{4}r\sin\Big(\frac{P_1}{2}+\frac{\sqrt{3}Q_1}{2}\Big),\quad Q_2=Q_1-\frac{1}{4}r\sin\Big(\frac{P_1}{2}+\frac{\sqrt{3}Q_1}{2}\Big),$$

$$P_3=P_2-\frac{\sqrt{3}}{4}r\sin\Big(\frac{P_2}{2}+\frac{\sqrt{3}Q_2}{2}\Big),\quad Q_3=Q_2-r\sin(P_2),\quad Q_4=Q_3-\frac{1}{4}r\sin\Big(\frac{P_3}{2}+\frac{\sqrt{3}Q_3}{2}\Big),$$

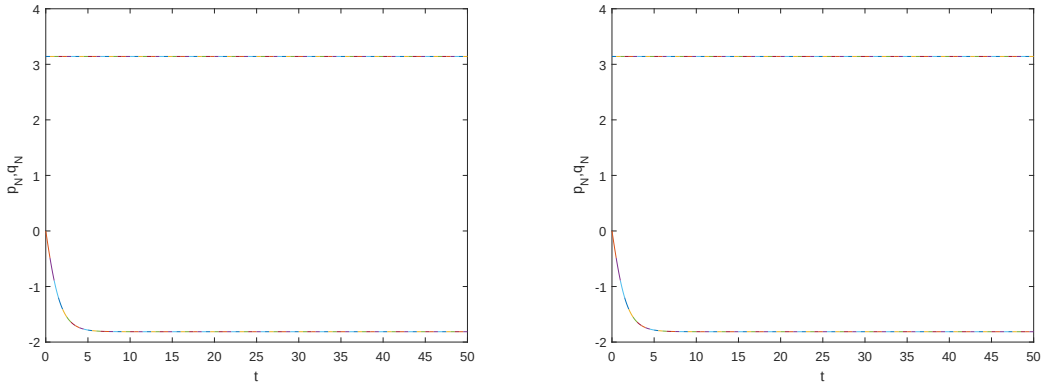

Figure 1: Graph of p_N (upper) and q_N (lower) versus t for $N=20$ (left), 30 (right).

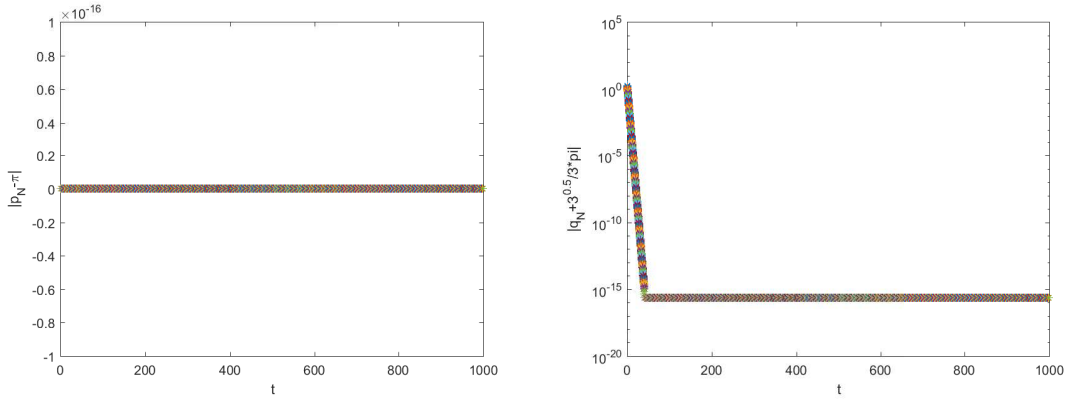

Figure 2: The error graphs between (p_N,q_N) and $(\pi,-\frac{\sqrt{3}}{3}\pi)$ versus t for $N=30$.

$$p^{k+1}=P_3+\frac{\sqrt{3}}{4}r\sin\Big(\frac{P_3}{2}+\frac{\sqrt{3}Q_4}{2}\Big),\quad q^{k+1}=Q_4-\frac{1}{4}r\sin\Big(\frac{P_3}{2}+\frac{\sqrt{3}Q_4}{2}\Big).$$

Compared with the symplectic method, the spectral Petrov-Galerkin method preserves the energy up to a high order accuracy and thus is more efficient in a long run. Note that even though both the spectral Petrov-Galerkin method and Lobatto collocation method have spectral accuracy, the drawback of the collocation method lies in that the differential matrices are usually full and the condition number of the matrix increases dramatically with increasing polynomial degrees. Large condition numbers lead to instability of the algorithm in some situations. While for the Petrov-Galerkin method, the differential matrix is diagonal and well conditioned. Therefore, as we may observe from Table 1, the spectral Petrov-Galerkin method proposed in this paper takes less CPU time and gives higher order accuracy than that of the symplectic method and the Lobatto spectral collocation method.

Table 1: Comparison of CPU times among three numerical methods.

Methods	time(secs)	Error in Energy
Spectral Petrov-Galerkin, $N=20$ on [0,1000]	3.72	0
Spectral Petrov-Galerkin, $N=20$ on [0,10000]	38.05	0
Lobatto collocation, $N=20$ on [0,1000]	33	$2.5368596112\times10^{-13}$
Lobatto collocation, $N=30$ on [0,10000]	2725(45mins)	$2.7539082125\times10^{-12}$
Symplectic, $r=0.001$ on [0,400]	2190	$6.425967063916294\times10^{-3}$
Symplectic, $r=0.001$ on [0,600]	5360(89mins)	$1.0537382086\times10^{-2}$

Example 5.2. The Toda system [13]. The Hamiltonian function of the Toda system is given by

$$H(p_1,p_2;q_1,q_2)=\frac{1}{2}(p_1^2+p_2^2)+\frac{1}{24}[e^{2q_2+2\sqrt{3}q_1}+e^{2q_2-2\sqrt{3}q_1}+e^{-4q_2}]-\frac{1}{8}.$$

The corresponding nonlinear Hamiltonian system is

$$\begin{aligned}
p_1'(t)&=-\frac{\partial H}{\partial q_1}=-\frac{\sqrt{3}}{12}(e^{2q_2+2\sqrt{3}q_1}-e^{2q_2-2\sqrt{3}q_1}),\\
p_2'(t)&=-\frac{\partial H}{\partial q_2}=-\frac{1}{12}(e^{2q_2+2\sqrt{3}q_1}+e^{2q_2-2\sqrt{3}q_1}-2e^{-4q_2}),\\
q_1'(t)&=\frac{\partial H}{\partial p_1}=p_1,\\
q_2'(t)&=\frac{\partial H}{\partial p_2}=p_2.
\end{aligned}$$

We choose the initial conditions $p_1(0)=0$, $p_2(0)=1$, $q_1(0)=1$, $q_2(0)=1$ and $r=0.1$. Again, there is no linear term in $H(p_1,p_2;q_1,q_2)$, which indicates the coefficients $c_0=c_1=0$ in Theorem 4.2. Note that $H(0)=10.221386879081575$ and

$$\begin{aligned}
&\frac{\partial^2 H}{\partial q_1^2}=\frac{1}{2}(e^{2q_2+2\sqrt{3}q_1}+e^{2q_2-2\sqrt{3}q_1}),\quad \frac{\partial^2 H}{\partial q_2^2}=\frac{1}{6}(e^{2q_2+2\sqrt{3}q_1}+e^{2q_2-2\sqrt{3}q_1}+4e^{-4q_2}),\\
&\frac{\partial^2 H}{\partial q_1 q_2}=\frac{\sqrt{3}}{6}(e^{2q_2+2\sqrt{3}q_1}-e^{2q_2-2\sqrt{3}q_1}),\quad \frac{\partial^2 H}{\partial p_i^2}=1,\quad \frac{\partial^2 H}{\partial p_1 p_2}=0,\quad \frac{\partial^2 H}{\partial p_i q_j}=0,\quad i,j=1,2.
\end{aligned}$$

On the other hand, using the energy conservation property yields

$$H(t)=\frac{1}{2}(p_1^2+p_2^2)+\frac{1}{24}[e^{2q_2+2\sqrt{3}q_1}+e^{2q_2-2\sqrt{3}q_1}+e^{-4q_2}]-\frac{1}{8}=H(0),$$

and thus

$$e^{2q_2+2\sqrt{3}q_1}+e^{2q_2-2\sqrt{3}q_1}+e^{-4q_2}\leq 24\Big(H(0)+\frac{1}{8}\Big).$$

Table 2: The energy $H(p_{1N},p_{2N};q_{1N},q_{2N})$ for different N and r at time $T=100$.

N	$r=\frac{1}{10}$	$r=\frac{2}{10}$	$r=\frac{1}{3}$	$r=\frac{2}{5}$	$r=\frac{1}{2}$
10	10.221386879082386	10.221386879083159	10.221386879084136	NaN	NaN
15	10.221386879082416	10.221386879083196	10.221386879083882	NaN	NaN
20	10.221386879082502	10.221386879083203	10.221386879084022	NaN	NaN
25	10.221386879082441	10.221386879083189	10.221386879083887	NaN	NaN

Table 3: The energy $H(p_{1N},p_{2N};q_{1N},q_{2N})$ at different time with $r=0.1$.

N	$t=10$	$t=100$	$t=1000$	$t=10000$
10	10.221386879081633	10.221386879082386	10.221386879090135	10.221386879167039
15	10.221386879081649	10.221386879082416	10.221386879090357	10.221386879167737
20	10.221386879081663	10.221386879082502	10.221386879090471	10.221386879167287
25	10.221386879081658	10.221386879082441	10.221386879090387	10.221386879167937

Consequently,

$$\begin{aligned}\kappa &= \max_{1\le i,j\le 2}\left(\left|\frac{\partial^2 H}{\partial p_i p_j}\right|,\left|\frac{\partial^2 H}{\partial q_i q_j}\right|,\left|\frac{\partial^2 H}{\partial p_i q_j}\right|\right)\\ &\le \frac{1}{2}(e^{2q_2+2\sqrt{3}q_1}+e^{2q_2-2\sqrt{3}q_1}+e^{-4q_2})+\frac{1}{6}e^{-4q_2}\le 16\Big(H(0)+\frac{1}{8}\Big).\end{aligned}$$

In this case, we have $\kappa=16(H(0)+\frac{1}{8})$, and then use the conclusion in Theorem 4.2 to obtain

$$r\le\frac{1}{8n\kappa}\approx 0.0004. \tag{5.3}$$

To demonstrate the effect of r on our iterative algorithm, we test different r in our numerical experiments. In Table 2, we present numerical results of the energy $H(p_{1N},p_{2N};q_{1N},q_{2N})$ for different N and r at time $T=100$. As indicated by Table 2, our algorithm is stable and convergent when $r\le\frac{1}{3}$. While $r\ge\frac{2}{5}$, the iterative scheme is divergent. In other words, the choice of r have an influence on the convergence and stability of our iterative scheme. Furthermore, it seems that the estimate for r in (5.3) or in Theorem 4.2 is not sharp.

In order to demonstrate the accuracy and efficiency of our algorithm, we choose the numerical solutions p_{iN}, q_{iN} $(i=1,2)$ with $N=60$ as our reference solution and plot in Fig. 6 the error curves of approximate solutions p_{iN}, q_{iN} $(i=1,2)$ for different N. Furthermore, we also list in Table 3 the energy $H(p_{1N},p_{2N};q_{1N},q_{2N})$ at different time for different N. We observe that, the energy error achieves at least thirteen-digit accuracy at time $t=10,100$ and eleven-digit accuracy at time $t=1000$, 10000 with $N\ge 20$. In other words, the Petrov-Galerkin method preserves the energy with a reasonable N.

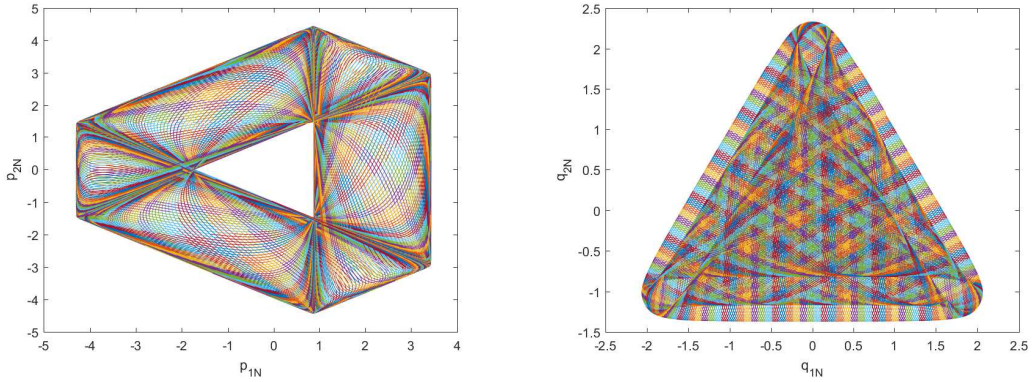

Figure 3: The phase plot p_{2N} versus p_{1N} (left) and q_{2N} versus q_{1N} (right) on $[0,1000]$ with $N=20$.

In Fig. 3, we also represent the phase plots of p_{2N} versus p_{1N} (left) and q_{2N} versus q_{1N} (right) on $[0,1000]$ with $N=20$. From Fig. 3 we see that the spectral Petrov-Galerkin method can keep trajectory stability for a long time.

Example 5.3. A modified Two-body problem [27,36].

The Hamiltonian function for this system is as follows:

$$H(\mathbf{p};\mathbf{q})=\frac{1}{2}\|\mathbf{p}\|^2-\frac{1}{\|\mathbf{q}\|}-\frac{\epsilon}{2\|\mathbf{q}\|^3},$$

where ϵ is a small perturbation parameter and $(\mathbf{p};\mathbf{q})=(p_1,p_2;q_1,q_2)$. In other words, the nonlinear Hamiltonian system is given by

$$\begin{aligned}
p_1'(t)&=-\frac{q_1}{\sqrt{(q_1^2+q_2^2)^3}}-\frac{3\epsilon q_1}{2\sqrt{(q_1^2+q_2^2)^5}},\\
p_2'(t)&=-\frac{q_2}{\sqrt{(q_1^2+q_2^2)^3}}-\frac{3\epsilon q_2}{2\sqrt{(q_1^2+q_2^2)^5}},\\
q_1'(t)&=p_1(t),\\
q_2'(t)&=p_2(t),
\end{aligned}$$

with initial conditions $\mathbf{p}(0)=(p_{10},p_{20})$, $\mathbf{q}(0)=(q_{10},q_{20})$. In addition to energy conservation, this system also preserves the angular momentum. That is, $p^TJq(t)=p^TJq(0)$ for any $t>0$, or equivalently, $\frac{d(p^TJq)}{dt}=0$. In our experiment, we take $\epsilon=0.005$, $r=1$ and choose the initial value $(\mathbf{p}(0),\mathbf{q}(0))=(0,\sqrt{\frac{1+e}{1-e}},1-e,0)$ with $e=0.001$, where e is the eccentricity of the orbit.

We list in Tables 4-5 the numerical results of the energy $H(\mathbf{p}_N;\mathbf{q}_N)$ and the angular momentum $(\mathbf{p}_N)^TJ\mathbf{q}_N$ at different time for different N, respectively. We observe that

Table 4: The energy $H(\mathbf{p}_N(t);\mathbf{q}_N(t))$ at different time for different N with $\epsilon=0.005$.

N	$t=10$	$t=100$	$t=1000$	$t=10000$
10	-0.502507515025034	-0.502507515024999	-0.502507515024640	-0.502507515021092
15	-0.502507515025034	-0.502507515024998	-0.502507515024650	-0.502507515021115
20	-0.502507515025034	-0.502507515024999	-0.502507515024645	-0.502507515021090
25	-0.502507515025034	-0.502507515025000	-0.502507515024644	-0.502507515021077

Table 5: The angular momentum $(\mathbf{p}_N)^T J\mathbf{q}_N$ at different time for different N with $\epsilon=0.005$.

N	$t=10$	$t=100$	$t=1000$	$t=10000$
10	-0.999999499999879	-0.999999499999914	-0.999999500000266	-0.999999500003761
15	-0.999999499999878	-0.999999499999914	-0.999999500000257	-0.999999500003739
20	-0.999999499999878	-0.999999499999913	-0.999999500000261	-0.999999500003763
25	-0.999999499999878	-0.999999499999912	-0.999999500000263	-0.999999500003776

both the energy $H(\mathbf{p}_N;\mathbf{q}_N)$ and the angular momentum $(\mathbf{p}_N)^T J\mathbf{q}_N$ can achieve at least thirteen-digit accuracy at time $t=10,100$ and eleven-digit accuracy at time $t=1000$, 10000 when $N\geq 20$. In other words, the spectral Petrov-Galerkin method at least preserves the energy and the angular momentum up to a numerically negligible error.

To further demonstrate the accuracy of our algorithms and the energy and angular momentum conserving properties, we plot in Fig. 4 the error curves of the energy $H(\mathbf{p}_N;\mathbf{q}_N)$ and angular momentum $(\mathbf{p}_N)^T J\mathbf{q}_N$ at different time for different N. We observe from Fig. 4 that the energy and angular momentum errors reach the machine precision for all N, which indicates that the spectral Petrov-Galerkin method preserves the energy and the angular momentum up to a high order accuracy.

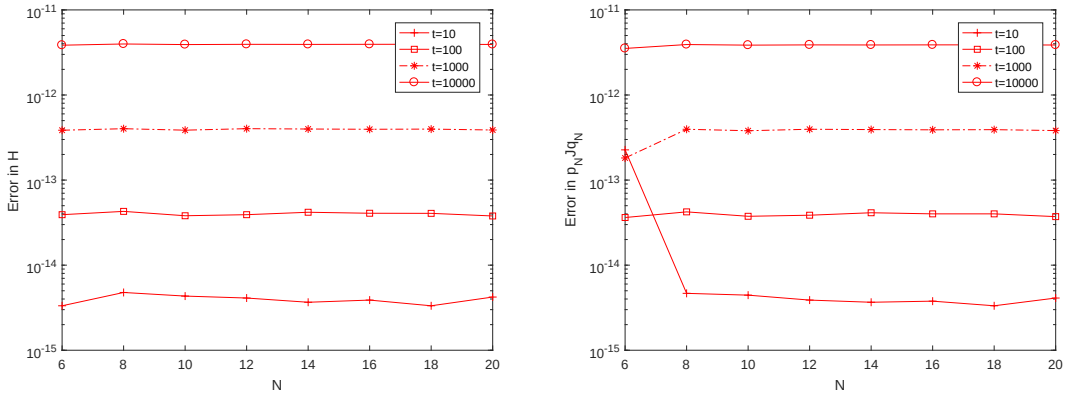

Figure 4: The error curves of the energy (left) and the angular momentum (right).

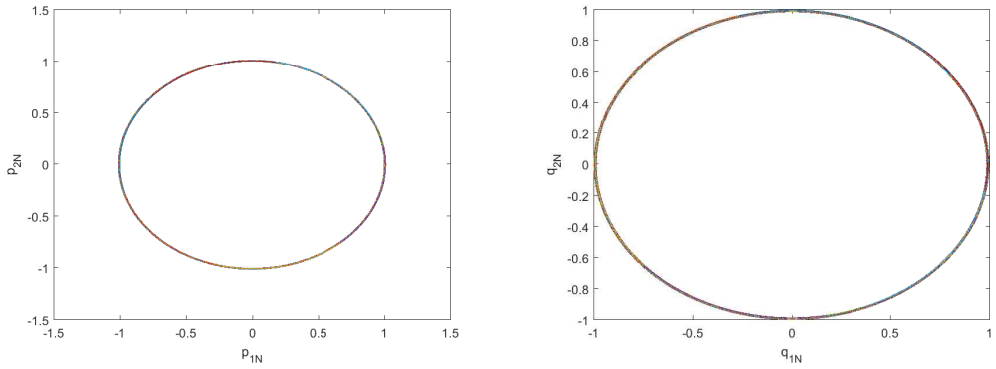

Figure 5: The phase plot p_{2N} versus p_{1N} (left) and q_{2N} versus q_{1N} (right) on $[0,10000]$ with $N=20$.

Table 6: Comparison of CPU times among the three methods with $\epsilon=0.005$.

Methods	time(secs)	Error in Energy
Spectral Petrov-Galerkin, $N=20$ on $[0,10000]$	93.21	$3.947842053264594\times10^{-12}$
Spectral Petrov-Galerkin, $N=20$ on $[0,1000]$	8.61	$3.922417946000678\times10^{-13}$
Collocation, $N=20$ on $[0,10000]$	4950	2.15614193×10^{-11}
Collocation, $N=20$ on $[0,1000]$	52	2.15372164×10^{-12}
Midpoint Euler, $r=0.001$ on $[0,75]$	53	6.05561933×10^{-8}
Midpoint Euler, $r=0.001$ on $[0,80]$	72	6.48879968×10^{-8}

In Fig. 5, we represent the phase plots of p_{2N} versus p_{1N} (left) and q_{2N} versus q_{1N} (right) on $[0,10000]$ with N=20, respectively. We observe that the spectral Petrov-Galerkin method can keep trajectory stability for a long time.

To show the efficiency of our algorithm, we also compare in Table 6 the CPU times used for the spectral Petrov-Galerkin method with those for the Lobatto spectral collocation method and the symplectic methods (see [27]). Here the symplectic methods we used is a second order midpoint Euler scheme. That is,

$$p_i^{k+1}=p_i^{k+1}-rH_{q_i}\Big(\frac{\mathbf{p}^{k+1}+\mathbf{p}^k}{2},\frac{\mathbf{q}^{k+1}+\mathbf{q}^k}{2}\Big),$$
$$q_i^{k+1}=q_i^{k+1}+rH_{p_i}\Big(\frac{\mathbf{p}^{k+1}+\mathbf{p}^k}{2},\frac{\mathbf{q}^{k+1}+\mathbf{q}^k}{2}\Big),\quad 1\le i\le n.$$

Again, we observe that the spectral Petrov-Galerkin proposed in this paper take less CPU time and give higher order of error than the other two methods, and thus are more effective in a long run.

Now we test the case $\epsilon=0$. Note that $\nabla H(\mathbf{p},\mathbf{q})$ is singular at the point $\mathbf{q}=(0,0)$. In other words, the Lipschitz condition (4.6) is not satisfied at $\mathbf{q}=(0,0)$. We consider the point near the singularity $\mathbf{q}=(0,0)$. In our numerical experiment, we take the initial value

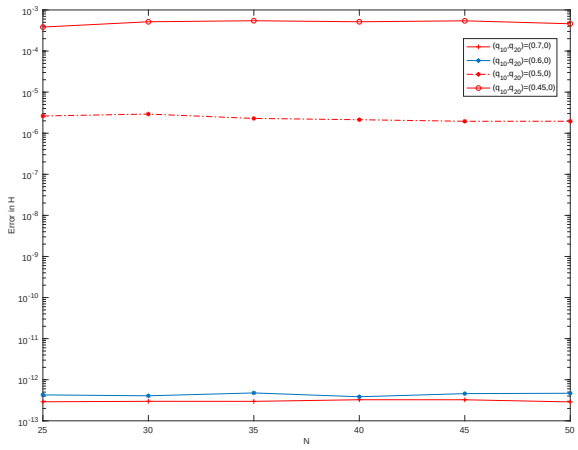

Figure 6: The energy $H(\mathbf{p}_N;\mathbf{q}_N)$ for different N and initial solution $\mathbf{q}(0)$ at time $T=1000$.

Table 7: Comparison of CPU times among the three methods with $\epsilon=0$.

Methods	time(secs)	Error in Energy
Spectral Petrov-Galerkin, $N=20$ on $[0,100]$	0.82	$3.375077994860476\times10^{-14}$
Lobatto collocation, $N=20$ on $[0,100]$	3	4.28660520×10^{-7}
Midpoint Euler, $r=0.001$ on $[0,40]$	75	3.02104066×10^{-7}
Midpoint Euler, $r=0.001$ on $[0,50]$	166	3.02104066×10^{-7}

$\mathbf{p}(0)=(0,\sqrt{\frac{1+e}{1-e}})$ and $\mathbf{q}(0)=(q_{10},0)$ with $q_{10}=0.7$, 0.6, 0.5, 0.45. Note that when q_{10} tends to zero, then κ in (4.6) goes to infinity. Plotted in Fig. 6 the error curves of the energy $H(\mathbf{p}_N;\mathbf{q}_N)$ for different N and different initial solutions $\mathbf{q}(0)$. We observe that the energy can reach the machine precision for all N in case $q_{10}=0.7$, 0.6. While for $q_{10}=0.5$, 0.45, the numerical method fails to keep the energy up to a high order accuracy even for large N. In other words, the Lipschitz condition (4.6) has effect on the accuracy and efficiency of the numerical methods. Moreover, the number of the iterative might depend on the initial solutions in this case. As q_{10} is close to zero, the time step size r is getting close to *zero* and the accumulation error becomes larger, then the iterative number increases and the instability of the algorithm might emerge.

To show the efficiency of our algorithm, we also compare in Table 7 the CPU times used for the spectral Petrov-Galerkin method with those for the Lobatto spectral collocation method and the symplectic methods (see [27]). We take the same initial solutions as that in [27]. That is, $\mathbf{p}(0)=(0.1,0.9)$, $\mathbf{q}(0)=(1,1)$. Again, we observe from Table 7 that the spectral Petrov-Galerkin method takes less CPU time and obtain higher accuracy than the symplectic methods and the Lobatto spectral collocation method.

Example 5.4. The Three-body system [23,27].

We consider the model which describes the motion of the satellite around the Earth and Moon. The Hamiltonian of the system is given by

$$H(p_x,p_y,x,y)=\frac{p_x^2+p_y^2}{2}+(yp_x-xp_y)-\Big(\frac{1-\mu}{r_1}+\frac{\mu}{r_2}\Big),$$

where $r_1^2=(x+\mu)^2+y^2$, $r_2^2=(x+\mu-1)^2+y^2$, (x,y) is the coordinate of the satellite and $\mu=0.01215$ (the length unit is 384400 km) is the mass of the Moon. The corresponding system of nonlinear ordinary differential equations for the Hamiltonian $H(p_x,p_y,x,y)$ is

$$p_x'(t)=p_y-\frac{(1-\mu)}{r_1^3}(x+\mu)-\frac{\mu}{r_2^3}(x+\mu-1), \tag{5.4}$$

$$p_y'(t)=-p_x-\frac{(1-\mu)}{r_1^3}y-\frac{\mu}{r_2^3}y, \tag{5.5}$$

$$x'(t)=p_x+y, \tag{5.6}$$

$$y'(t)=p_y-x. \tag{5.7}$$

Let $p_1=p_x+p_y$, $p_2=p_x-p_y$, $q_1=\frac{1}{2}(x+y)$, $q_2=\frac{1}{2}(x-y)$. Then the system (5.4)-(5.7) is equivalent to the following system:

$$\begin{aligned}
p_1'(t)&=-p_2-\frac{(1-\mu)(2q_1+\mu)}{[(q_1+q_2+\mu)^2+(q_1-q_2)^2]^{\frac{3}{2}}}-\frac{\mu(2q_1+\mu-1)}{[(q_1+q_2+\mu-1)^2+(q_1-q_2)^2]^{\frac{3}{2}}},\\
p_2'(t)&=p_1-\frac{(1-\mu)(2q_2+\mu)}{[(q_1+q_2+\mu)^2+(q_1-q_2)^2]^{\frac{3}{2}}}-\frac{\mu(2q_2+\mu-1)}{[(q_1+q_2+\mu-1)^2+(q_1-q_2)^2]^{\frac{3}{2}}},\\
q_1'(t)&=\frac{1}{2}(p_1-2q_2),\\
q_2'(t)&=\frac{1}{2}(p_2+2q_1).
\end{aligned}$$

To test the efficiency of our algorithm, we choose the same initial values of those in [27]. That is, $p_1(0)=1.259185$, $p_2(0)=-1.259185$, $q_1(0)=-0.25$, $q_2(0)=-0.25$. We list in Table 8 the energy $H(p_{1N},p_{2N};q_{1N},q_{2N})$ at different time for different N with $r=1$.

Table 8: The energy $H(p_{1N},p_{2N};q_{1N},q_{2N})$ at different time for different N.

N	$t=10$	$t=100$	$t=1000$	$t=10000$
10	-0.610705409937636	-0.610705409937179	-0.610705409932793	-0.610705409924976
15	-0.610705409937624	-0.610705409937180	-0.610705409932886	-0.610705409830834
20	-0.610705409937617	-0.610705409937198	-0.610705409932607	-0.610705409884133
25	-0.610705409937604	-0.610705409937156	-0.610705409932653	-0.610705409884112

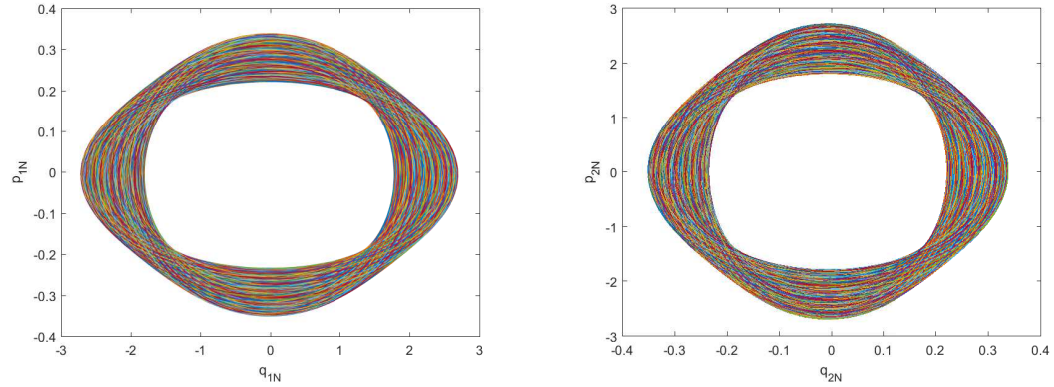

Figure 7: The phase plot q_{1N} versus p_{1N} (left) and q_{2N} versus p_{2N} (right) on $[0,10000]$ with $N=20$.

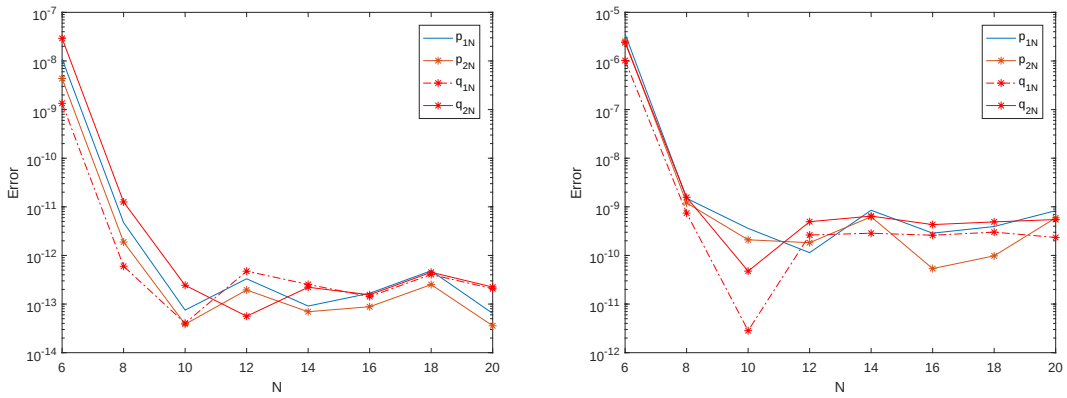

Figure 8: Errors graphs of approximate solutions p_{iN}, q_{iN} $(i=1,2)$ at $T=100$ (left) and $T=10000$ (right) for different N with $r=0.1$.

From Table 8 we see that the energy $H(p_{1N},p_{2N};q_{1N},q_{2N})$ achieves at least twelve-digit accuracy at time $t=10$, 100 and nine-digit accuracy at time $t=1000$, 10000 with $N\geq 20$. In other words, the Petrov-Galerkin method preserves the energy numerically.

We present in Fig. 7 the phase plots of q_{1N} versus p_{1N} (left) and q_{2N} versus p_{2N} (right) on $[0,10000]$ with $N=20$, respectively, which indicates that the spectral Petrov-Galerkin method can keep trajectory stability for a long time.

In Table 9, we compare the CPU times used for the Petrov spectral-Galerkin method with those for the Lobatto spectral collocation method (see [27]) and the symplectic midpoint Euler scheme. Just the same as that in Example 5.1 and Example 5.3, the spectral Petrov-Galerkin method takes less CPU time and gives higher order of error than the other two methods, which indicates the efficiency of our algorithm.

Table 9: Comparison of CPU times among the three methods.

Methods	time(secs)	Error in Energy
Spectral Petrov-Galerkin, $N=20$ on $[0,10000]$	250.62	$5.353717469347430\times10^{-11}$
Spectral Petrov-Galerkin, $N=20$ on $[0,1000]$	24.82	$5.062616992290714\times10^{-12}$
Spectral Petrov-Galerkin, $N=10$ on $[0,300]$	3.4	$1.409761973825141\times10^{-9}$
Collocation, $N=20$ on $[0,300]$	5.4	$1.9090052472\times10^{-7}$
Midpoint Euler, $r=0.001$ on $[0,300]$	18	$9.3757448742\times10^{-3}$
SMidpoint Euler, $r=0.001$ on $[0,150]$	4.6	$4.8046166186\times10^{-3}$

6 Conclusions

In this work, we analyze an efficient spectral Petrov-Galerkin time-stepping method for nonlinear Hamiltonian systems. Convergence of the iterative algorithm and applications of the algorithm to various Hamiltonian problems have been investigated. We established the stability condition for the iterative algorithm (see Section 4), and prove that the choice of time step size r is dependent on the specific properties of the Hamiltonian systems, e.g., n and the Hamiltonian function. The established stability condition helps us to efficiently take a suitable r when solving different Hamiltonian systems. Furthermore, numerical experiments show that our algorithm preserves the energy up to a machine precision with a reasonable polynomial degree N, and preserves symplectic structure better. Comparing with the existing symplectic methods or low order Galerkin methods, the proposed Petrov-Galerkin method has high-order accuracy and hence requires less CPU time for obtaining the same order accuracy, and predicts more accurate trajectories for long large time t and thus are more efficient. Our current and future works include the study of the applications of our algorithm as an efficient time discretization method to some partial differential equations, e.g., Cahn-Hilliard problems, which could be more challenging and interesting.

Acknowledgments

This research was supported in part by NSFC grant No. 11726604, No. 11726603, No. 11871106, No. 11661022, No. 11871092, and NSAF grant U1530401, and the Guizhou Provincial Science and Technology Foundation No. [2017]1124, and the fundamental Research Funds for the Central Universities No. 2017NT10.

References

[1] J. An, W. Cao, and Z. Zhang, A class of efficient spectral methods and error analysis for nonlinear Hamiltonian systems, *preprint*.

[2] T. J. Bridges and S. Reich, Numerical methods for Hamiltonian PDEs, *Journal of Physics A: mathematical and general*, 39 (2006), 5287.
[3] J. P. Boyd, *Chebyshev and Fourier Spectral Methods*, Springer-Verlag, Berlin, 1989.
[4] C. Canuto, M. Y. Hussaini, A. Quarteroni, and T. A. Zang, *Spectral Methods in Fluid Dynamics*, Springer-Verlag, Berlin, 1988.
[5] J. Candy and W. Rozmus, A symplectic integration algorithm for separable Hamiltonian functions, *J. Comput. Phys.*, 92 (1991), pp. 230-256.
[6] P. J. Channell, *Symplectic Integration Algorithms*, Los Alamos National Laboratory Report AT-6:ATN 83-9 (1983).
[7] D. Cohen, L. Gauckler, E. Hairer, and C. Lubich, Long-term analysis of numerical integrators for oscillatory Hamiltonian systems under minimal non-resonance conditions, *BIT* 55 (2015), pp. 705-732.
[8] D. Cohen, E. Hairer, and C. Lubich, Numerical energy conservation for multi-frequency oscillatory differential equations, *BIT Numer. Math.*, 45 (2005), pp. 287-305.
[9] E. Faou, E. Hairer, and T. L. Pham, Energy conservation with non-symplectic methods: examples and counter-examples. *BIT Numer. Math.*, 44 (2004), pp. 699-709.
[10] K. Feng, *On difference schemes and symplectic geometry. In: Proceedings of the 5th international symposium on differential geometry and differential equations,* 1984.
[11] K. Feng, *How to compute properly Newton's equation of motion. In: Proceedings of 2nd Conference on Numerical Methods for Partial Differential Equations,* World Scientific, Singapore, 1992, pp. 15-22.
[12] K. Feng, *The Hamiltonian way for computing Hamiltonian dynamics. In: Applied and Industrial Mathematics,* Springer, Dordrecht, 1991, pp. 17-35.
[13] K. Feng and M. Qin, *Symplectic Geometric Algorithms for Hamiltonian Systems,* Springer, Berlin, 2010.
[14] D. Gottlieb and S. A. Orszag, *Numerical Analysis of Spectral Methods: Theory and Applications*, SIAM-CBMS, Philadelphia, 1977.
[15] B.-Y. Guo, *Spectral Methods and their Applications*, World Scientific, Singapore, 1998.
[16] B.-Y. Guo and Q.-Z. Wang, Legendre-Gauss collocation methods for ordinary differential equations, *Adv. Comput. Math.*, 30 (2009), pp. 249-280.
[17] E. Hairer and C. Lubich, Long-time energy conservation of numerical methods for oscillatory differential equations, *SIAM J. Numer. Anal.*, 38 (2000), pp. 414-441.
[18] E. Hairer and C. Lubich, *Oscillations over long times in numerical Hamiltonian systems, in Highly oscillatory problems (B. Engquist, A. Fokas, E. Hairer, A. Iserles, eds.),* London Mathematical Society Lecture Note Series 366, Cambridge Univ. Press, 2009.
[19] E. Hairer, C. Lubich and G. Wanner, *Geometric Numerical Integration. Structure-Preserving Algorithms for Ordinary Differential Equations,* 2nd ed., Springer Science in Computational Mathematics 31, Springer-Verlag, Berlin, 2006.
[20] R. A. Labudde and D. Greenspan, Energy and momentum conserving methods of arbitrary order for the numerical integration of equations of motion, Part I, *Numer. Math.*, 7 (1976), pp. 323-346.
[21] F. M. Lasagni, Canonical runge-kutta methods, *Zeitschrift für Angewandte Mathematik und Physik (ZAMP)*, 39 (1988), pp. 952-953.
[22] B. Leimkuhler and S. Reich, *Simulating Hamiltonian Dynamics*, Cambridge University Press, 2004.
[23] W. Lu, H. Zhang, and S. Wang, Application of symplectic algebraic dynamics algorithm to circular restricted three-body problem, *Chin. Phys. Lett.*, 25 (2008), pp. 2342-2345.

[24] J. E. Marsden, G. Misiolek, J. P. Ortega, M. Perlmutter, and T. S. Ratiu, *Hamiltonian reduction by stages,* Springer, 2007.
[25] J. E. Marsden and M. West, Discrete mechanics and variational integrators, *Acta Numerica*, 10 (2001), pp. 357-514.
[26] R. I. McLachlan and P. Atela, The accuracy of symplectic integrators, *Nonlinearity*, 5 (1992), pp. 541.
[27] K. Nanyamee and Z. Zhang, Comparison of a spectral collocation method and symplectic methods for Hamilton systems, *International Journal of Numerical Analysis and Modeling*, 8 (2011), pp. 86-104.
[28] R. D. Ruth, A Canonical Integration Technique, *IEEE Trans. Nucl. Sci.*, 30 (1983), pp. 1669-2671.
[29] J. M. Sanz-Serna, Runge-Kutta schemes for Hamiltonian systems, *BIT Numer. Math.*, 28 (1988), pp. 877-883.
[30] J. M. Sanz-Serna and M. P. Calvo, *Numerical Hamiltonian Problems,* Courier Dover Publications, 2018.
[31] J. Shen, T. Tang, and L. L. Wang, *Spectral Methods: Algorithms, Analysis and Applications,* Springer Science and Business Media, 2011.
[32] J. Shen and L. L. Wang, Fourierization of the Legendre-Galerkin method and a new space-time spectral method, *Applied Numerical Mathematics*, 57 (2007), pp. 710-720.
[33] J. Shen, Efficient spectral-Galerkin method I. Direct solvers of second-and fourth-order equations using Legendre polynomials, *SIAM J. Sci. Comput.*, 15 (1994), pp. 1489-1505.
[34] J. C. Simo, N. Tarnow, and K. K. Woog, Exact energy-momentum conserving algorithms and symplectic schemes for nonlinear dynamics, *Comput. Methods Appl. Mech. Engrg.*, 1 (1992), pp. 63-116.
[35] Q. Tang, C. Chen, and L. Liu, Energy conservation and symplectic properties of continuous finite element methods for Hamiltonian systems, *Applied mathematics and computation*, 181 (2006), pp. 1357-1368.
[36] H. Van deVyver, A fourth-order symplectic exponentially fitted integrator, *Computer Phys. Comm.*, 174 (2006), pp. 255-262.
[37] T. Wihler, An *a priori* error analysis of the hp-version of the continuous Galerkin FEM for nonlinear initial value problems *J. Sci. Comput.*, 25 (2005), pp. 523-549.
[38] G. Zhong and J. E. Marsden, Lie-Piosson Himilton-Jacobi theory and Lie-Poisson integrators, *Phys. Lett. A.*, 133 (1988), pp. 134-139.